Engineering 28 (2023) 79–92

Contents lists available at ScienceDirect

Engineering

journal homepage: www.elsevier.com/locate/eng

Research
Geotechnical Engineering—Article

The Geoscience Frontier of Gulong Shale Oil: Revealing the Role of Continental Shale from Oil Generation to Production

Wenyuan He [a,c,#], Rukai Zhu [b,#], Baowen Cui [c,d], Shuichang Zhang [b], Qian Meng [c,d], Bin Bai [b], Zihui Feng [c,d], Zhengdong Lei [b], Songtao Wu [b], Kun He [b], He Liu [b,c], Longde Sun [c,e,*]

[a] China National Oil and Gas Exploration and Development Company Ltd., Beijing 100027, China
[b] Research Institute of Petroleum Exploration and Development, PetroChina, Beijing 100083, China
[c] Key Laboratory of Shale Oil Accumulation of Heilongjiang Province, Daqing 163712, China
[d] Daqing Oilfield Company Ltd., PetroChina, Daqing 163712, China
[e] China National Petroleum Corporation, Beijing 100007, China

ARTICLE INFO

Article history:
Received 14 June 2022
Revised 13 August 2022
Accepted 31 August 2022
Available online 2 January 2023

Keywords:
Gulong shale
Gulong shale oil
Micro-nano pores
Lamellar fracture
Continental oil production

ABSTRACT

The clay mineral content of Daqing Gulong shale is in the range of about 35%–45%, with particle sizes less than 0.0039 mm. The horizontal fluidity of oil in Gulong shale is poor, with near-zero vertical flowability. As a result, Gulong shale has been considered to lack commercial value. In recent years, however, interdisciplinary research in geoscience, percolation mechanics, thermodynamics, and surface mechanics has demonstrated that Gulong shale oil has a high degree of maturity and a high residual hydrocarbon content. The expulsion efficiency of Gulong shale in the high mature stage is 32%–48%. Favorable storage spaces in Gulong shale include connecting pores and lamellar fractures developed between and within organic matter and clay mineral complexes. The shale oil mainly occurs in micro- and nano-pores, bedding fractures, and lamellar fractures, with a high gas–oil ratio and medium–high movable oil saturation. Gulong shale has the characteristics of high hardness, a high elastic modulus, and high fracture toughness. This study achieves breakthroughs in the exploration and development of Gulong shale, including the theories of hydrocarbon generation and accumulation, the technologies of mobility and fracturing, and recoverability. It confirms the major transition of Gulong shale from oil generation to oil production, which has extremely significant scientific value and application potential for China's petroleum industry.

1. Introduction

Few scientists believed that commercial oil resources could be generated from non-marine sedimentary systems. In 1942, Pan put forward the new concept of "terrestrial origin of petroleum" for the first time in an article titled "Geological notes: non-marine origin of petroleum in north Shensi and the Cretaceous of Szechuan, China" published in the *American Association of Petroleum Geologists (AAPG) Bulletin* [1], and thereby provided a scientific basis for oil discovery in China's continental basins. The first large-scale oil field discovered in terrestrial facies was the Daqing Oilfield in the Songliao Basin, in the late 1950s. After 60 years of exploration and development, the proven geological reserves of conventional oil in the Daqing Oilfield are 6.37×10^9 tonnes [2,3], and the cumulative oil production is 2.399×10^9 tonnes [4]. Currently, recovery from major oil fields has reached 52.2%, recovery of recoverable reserves has reached 92.33%, the comprehensive water cut of the Changyuan Oilfield has reached 95.92% [4,5], and the proven rate of conventional oil in the Daqing Oilfield has reached 68.35%. New questions are now arising: Are there any other new oil resources? If so, where are they, and how can they be found and developed? With the concept of "looking for a new Daqing Oilfield below and outside of the Daqing Oilfield," the people working at Daqing are trying to find new oil and gas resources. The Qingshankou Oilfield Formation's shale has been established as a new target for research, and the newly completed Well Guyeyoping 1 drilled in the formation has revealed new insights.

The concept of "shale oil" is well known in industry and academia. Nearly a hundred years ago, in 1929, the Chinese geologist Xie divided oil shale into two types in his book *Petroleum*: One type is

* Corresponding author.
E-mail address: sunld-tlm@petrochina.com.cn (L. Sun).
# These authors contributed equally to this work.

https://doi.org/10.1016/j.eng.2022.08.018

shale that is saturated with oil, and the other is shale without oil—although, after distillation, the organic matter in the latter form of shale can still combine to form oil [6]. The first of these types is now known as shale oil. However, shale oil was not properly explored and exploited until this century, particularly in the last ten years. The shale oil and gas revolution, which has mainly involved marine shales in the United States, has greatly increased that country's oil and gas self-sufficiency rate, changed the global oil and gas supply–demand structure, and had a profound impact on world geopolitics [7–12].

As early as the 1960s, signs of oil and gas (SO&G) were found in many wells in the Qingshankou Formation shale. It was found that oil seeps along the bedding planes [13]. In the Daqing Oilfield, a series of industrial practices, divided into three periods, have been carried out to test the production capacity of the shale. In the first period (1981–1997), vertical wells were used to extract oil from conventional reservoirs with mudstone fractures. Exploration during this period confirmed the oil-bearing properties of the mudstone fractures and recognized their complexity and strong heterogeneity. In the second period (1998–2011), horizontal wells and volume fracturing were adopted to extract oil from tight sandstone reservoirs mixed with thin layers in the shales. In the initial production period, the oil production of the tight sandstone reservoirs mixed with thin layers was increased by using horizontal wells. However, the exploration results were ultimately poor due to the thin reservoirs, limited resources, and unstable production. In the third period (2012–current date), the pure shale reservoirs are being explored by combining horizontal wells and large-scale composite volume fracturing [3,5]. In 2012, Wells Ying57x and Ying58x were deployed in Longhupao Terrace for the shale reservoir in the Qingshankou Formation. The wells were completed in March and April 2013, respectively, and their daily oil production was 3.3 and 6.7 tonnes, respectively. In 2018, researchers used innovative new concepts in oil exploration, studied and deployed the source layers as reservoirs, and drilled Well Guye 1 in the lower part of the Gulong Sag. Systematic coring of the shale in the Qingshankou Formation established that the cumulative thickness of oil layers above class I was 133 m. Daily oil production after fracturing was 2.5 tonnes, and vertical single-layer testing confirmed the oil production capacity in multiple oil layers in the shale of the Qingshankou Formation. In 2019, Well Guyeyouping 1 was deployed in the shale layer with high organic content at the bottom of Well Guye 1, and the horizontal section length of Well Guyeyouping 1 was 1562 m. High-yield industrial oil and gas flow with a daily oil production of 30.5 tonnes and daily gas production of 13 032 m^3 was achieved in Well Guyeyouping 1. After two years of oil production, the daily oil production was stable at about 10 m^3, and the cumulative oil production exceeded 1×10^4 m^3, thus representing a major historic strategic breakthrough. After the breakthrough in Well Guyeyouping 1, wells were intensively drilled in the Qijia–Gulong light oil belt, including 47 vertical test wells. Testing in these wells found oil traces in every well and layer. The single-layer tests showed oil production in all the layers. Nine horizontal wells were tested and obtained high production of more than 10 m^3. Among them, four wells had a daily oil production of more than 30 m^3, and production from the production wells was relatively stable. Recently, many horizontal wells have been upgraded and optimized using fracturing, drainage, and recovery technologies. These new horizontal wells are characterized by the high production. The initial daily oil production was more than 20 m^3. After around three months of production, formation pressure remained high. Based on theoretical understanding and drilling findings, shale oil resources with an area of more than 1×10^4 m^3 were evaluated in the middle-high maturity area of the Qingshankou Formation in the northern Songliao Basin. The oil resources in the light oil belt of the Qijia–Gulong Sag were calculated to be 5.500×10^9 tonnes, and the newly increased predicted oil in place was 1.268×10^9 tonnes. Based on these discoveries, a national continental shale oil demonstration zone was established in Gulong, Daqing, and research determined that the continental pure shale strata is capable of producing industrial oil flows.

North American shale oil is mainly produced from late Paleozoic–Mesozoic marine sedimentary strata. The main lithologies of the marine sedimentary strata are fine sandstones, dolomitic siltstones, dolostones, and marls, which have high porosity and permeability and a clay mineral content of generally less than 30%. For example, the clay mineral content of the Bakken Formation in the Williston Basin of the United States is 21.5%, that of the Eagle Ford Formation in the West Bay Basin is 15.0%–30.0%, that of the Wolfcamp Formation in the Permian Basin is about 10%, that of the Barnett Formation is 24.2% on average, that of the Douwen Formation in the Western Canada Basin is about 26.0%, that of the Vaca Muerta Formation in the Neuquen Basin in Argentina is 10.0%–20.0%, and that of the Bazhenov Formation in the Siberian Basin is about 2.0%–27.0%. The content of brittle minerals can reach 60.0%–80.0%. All of these data confirm the high fracturing properties of shale [14–16].

Currently, the lithological combinations of shale oil belts that have been explored and developed in China are similar to those in North America. China's shale oil mainly comes from tight sandstones, siltstones, and lacustrine carbonate interlayers. For example, the shale oil layers of the Chang 7 Member in the Ordos Basin are mainly composed of siltstone and fine sandstone layers in the Chang 7^1 and Chang 7^2 Members. The clay mineral content is less than 20.0% [17,18]. The shale oil layers of the Lucaogou Formation in the Jimusar Sag in the Junggar Basin are mainly composed of silty dolomite and dolomitic siltstone, and the clay mineral content is less than 25.0% [19]. The main lithologies of the Kong 2 Member in the Cangdong Sag in the Bohai Bay Basin are felsic shale and mixed shale, and the average clay mineral content is 15.7% [20–22]. The main lithologies of the Shahejie Formation in the Jiyang Depression of the Bohai Bay Basin are laminar argillaceous limestone and calcareous mudstone, and the clay mineral content is 20.0%–30.0% [23,24]. The Paleogene Lower Ganchaigou Formation in the Qaidam Basin is mainly composed of grey dolomitic shale, and the clay mineral content is 10.0%–40.0% [25]. The clay mineral content in the Second Member of the Jurassic Daanzhai Formation of the Sichuan Basin is 21.0%–39.0%, with an average of 17.0% [26]. The content of clay minerals in the lacustrine shale of the Lianggaoshan Formation in Well Ping'an 1 is relatively high, with an average of 44.3%–48.6% [27]. However, Gulong shale oil is different from the shale oil at home and abroad, having been produced from the interbedded or transitional lithologic combination of tight sandstone, mixed rock, or carbonate rock. Gulong shale oil is mainly produced from clay minerals components which have higher oil contents, better storage spaces, and better fracability and could be first choice for engineering sweet spot [2,3,28–30]. As a result, during the exploration and development of Gulong shale oil, it is difficult to imitate and copy the theories, methods, and technologies developed for shale oil exploration at home and abroad (Table 1).

Gulong shale oil in the Songliao Basin mainly occurs in micro-nano pores, bedding fractures, and lamellar fractures, with poor plane and vertical fluidities [31,32]. The shale is black shale with a thickness of more than 100 m, which has excellent hydrocarbon generation potential and provides large amounts of hydrocarbons for conventional oil and gas fields. However, there is few knowledge on several scientific problems, such as hydrocarbon retention, occurrence space and facies, the oil accumulation and oil preservation in the shale systems, and no consensus has been reached at the industrial application problems, such as the petroleum resource potential and industrial production. Based on a large number of experimental analyses and a great deal of production data—especially detailed experimental data from the three

Table 1
Differences between Gulong shale oil and other shale oils in China and North America.

Parameter	Depth (m)	Lithology	Clay mineral content (%)	Thickness (m)	Kerogen type	TOC (%)	HI ($mg·g^{-1}$) TOC	OSI ($mg·g^{-1}$) TOC	S_1 ($mg·g^{-1}$)	R_o (%)	T_{max} (°C)	Peak carbon	Pressure coefficient (C_P)
Cretaceous Gulong shale	1500–2600	Clay rich shales	40–60	100–150	I	1.5–4.0	600–850	50–600	4.0–15.0	0.75–1.70	400–445	C_8	1.20–1.60
Permian Lucaogou Formation	1800–4000	Dolomitic sandstones, dolostones, and shales	< 20	15–35	I, II_1	1.5–9.0	200–800	—	3.0–12.0	0.55–1.10	420–460	C_{17}	1.10–1.30
Triassic Chang 7 member	1500–3000	Tight sandstones and shales	30–50	15–35	II	3.0–16.0	100–400	20–300	1.5–9.0	0.75–1.20	430–460	C_{15}, C_{16}	0.75–0.85
Devonian Bakken shale	2590–3200	Tight sandstones and dolomitic sandstones	< 30	5–12	II	10.0–15.0	50–600	25–100	3.0–5.0	0.60–1.20	425–445	—	1.35–1.50
Cretaceous Eagle Ford shale	914–4267	Marl and shales	< 10	20–60	II	3.0–7.0	200–650	50–150	0.5–4.5	0.70–1.30	415–455	—	1.35–1.80

TOC: total organic carbon; HI: hydrogen index; OSI: oil saturation index; S_1: free hydrocarbon content from rock eval analysis; R_o: vitrinite reflectance.

full-coring wells of Well Guye 2HC, Guye 3HC, and Guye 8HC—this study analyzes the generation, expulsion and retention, storage space, occurrence state, and flow mechanism of Gulong shale oil, revealing the entire process from generation to production for continental shale oil. This study is of great scientific significance and industrial value for the global production and efficient production of similar continental shale oils.

2. Geological background, lithology, and mineralogy

During the sedimentary period of the Qingshankou Formation, the Songliao Basin's structure settled into a stable state. The lake basin had a massive size with a water depth of more than 30 m. It was mostly deposited as continental saltwater/semi-deep freshwater lake/deep lake facies. Shale with a high clay content was stably distributed regionally in the lake basin, as supplies from onshore sources were transported for long distances and had little impact on the interior of the lake basin. Previous studies have shown that organic matter accumulates more easily and is better preserved in sedimentary environments with fresh water, warmth and humidity, reduction, insufficient terrigenous clastic supply, and volcanic eruption events. Some studies have concluded that the middle and upper parts of the first member of the Qingshankou Formation were deposited in a stable, highly saline, brackish environment and that the lower part was deposited in a brackish-saline to saline environment with layered salinity. The rapid increase of salinity in the Qingshankou Formation on the short term could be related to periodic transgression events [33–37]. The sedimentary area of the First Member of the Qingshankou Formation is 8.7×10^4 km^2, and the sedimentary area of the semi-deep lake/deep lake facies is greater than 3.0×10^4 km^2. The lake basin in the Second Member of the Qingshankou Formation shrank gradually from 90.1 Ma, and the sedimentary area decreased to 5.4×10^4 km^2. The sedimentary area of the Third Member of the Qingshankou Formation is decreased into 3.5×10^4 km^2.

Currently, based on the sedimentary cycles, lithological characteristics, mineral compositions, and total organic carbon (TOC) contents, the strata from the First Member to the lower part of the Second Member in the Qingshankou Formation can be further divided into nine layers (Q_1–Q_9) from bottom to top, with a cumulative thickness of 100–150 m (Fig. 1).

Gulong shale is mainly composed of shale, which accounts for more than 95% of the total thickness. The shale generally consists of fine-grained (< 0.0039 mm) clastic minerals such as quartz, clay mineral, feldspar, and small amounts of calcite. The clay mineral content is generally high, the carbonate mineral content is low, and the felsic mineral content is high. The shale is mixed with thin-layer siltstone, dolomite, and shell limestone, with the thickness of a single layer generally being 1–5 cm. For example, the Q_1 oil layer is 14.6 m thick, including 51 layers of grey–black shale with a total thickness of 13.36 m, eight layers of siltstone with a thickness of 0.52 m, four layers of dolomite with a thickness of 0.49 m, and a layer of shell limestone 0.23 m thick. The organic carbon content of the Q_1 layer is 0.8%–4.5% with an average of 2.6%, and the lamellar density is 2000–3000 pieces·m^{-1} [30].

A mineral content analysis of Well Guye 2HC (Fig. 2) reveals quartz contents of 26%–32% and feldspar contents of 15%–30%, which do not change significantly across the analysis. However, the contents of dolomite (6%–75%) and calcite (5%–30%) vary significantly. The clay content is 35%–45%, including illite (19%–80%, with an average of 68%), an illite-montmorillonite compound layer (9%–36%, with an average of 17%), and chlorite (5%–71%, with an average of 14%). The plane distribution shows that the proportion of illite in the clay minerals slightly decreases from Well Guye 1 to Well Guye 2HC and to Well Guye 3HC.

A mineral content analysis shows that the Gulong shale is mainly composed of felsic shale, clayey shale, and mixed shale (Fig. 3). Of these, the TOC content of the clay shale is relatively high. The mineral compositions in vertical single-well facies are relatively constant, with only the carbonate mineral content changing significantly. The Q_1–Q_6 Members are mainly composed of clay shale and mixed shale. Felsic shale increases in the Q_7–Q_9 Members (Fig. 4). In the plane distribution of lithofacies in Wells Guye 1, Guye 8HC, Guye 2HC, and Guye 3HC, these three lithofacies change little. The clay mineral content of Well Guye 1 in the central lake basin increases. In the first member of the Qingshankou Formation, mixed shale is the most developed, accounting for 37%–40%, with clay shale accounting for 32%–40% and felsic shale accounting for only 15%–22%.

3. Organic geochemistry

The source rock in the Qingshankou Formation of the Songliao Basin has high organic matter abundance (TOC contents mostly more than 2%) and is one of the major source rocks in China's

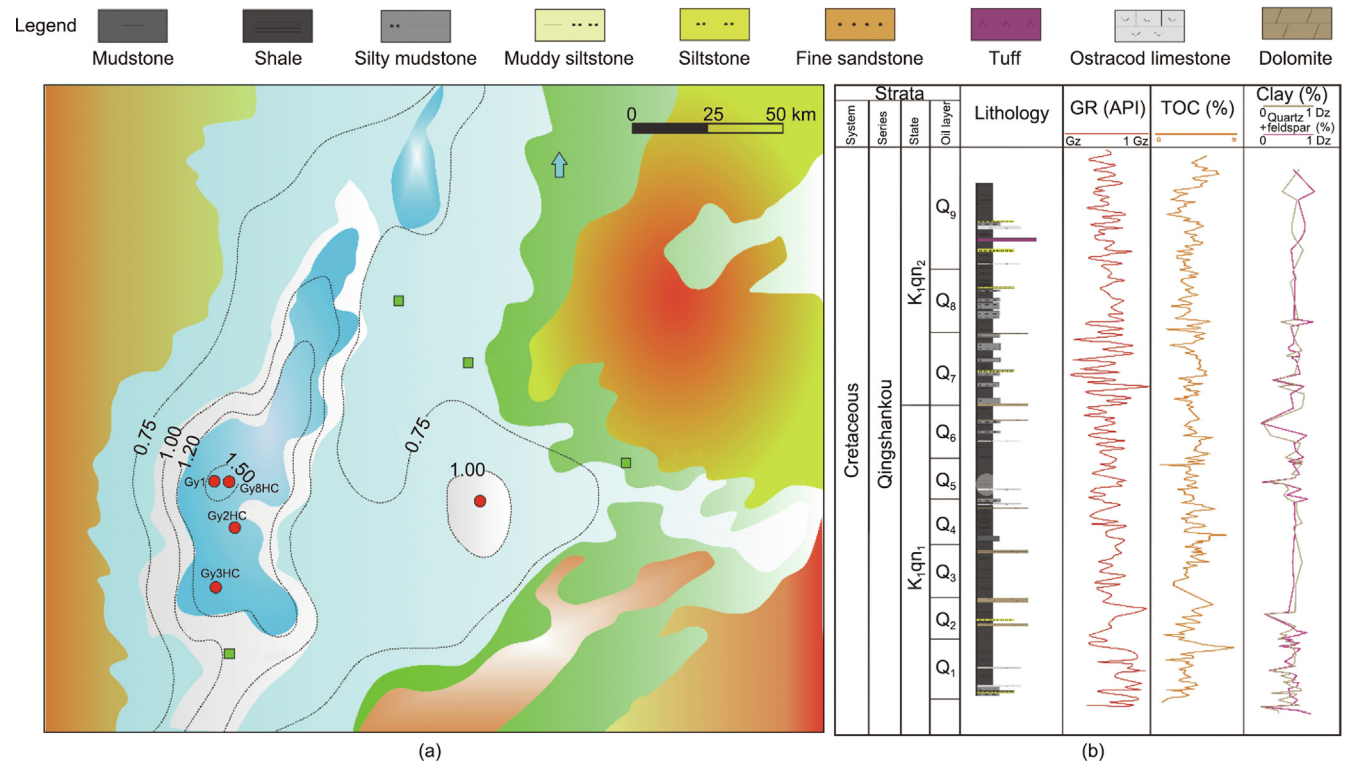

Fig. 1. Comprehensive column of the Cretaceous strata in the Songliao Basin. (a) Location of key wells in Gulong Sag and (b) lithology, TOC, and mineralogy of Well Guye 3HC. K_1: lower Cretaceous; qn: Qingshankou Formation; GR: Gamma ray log.

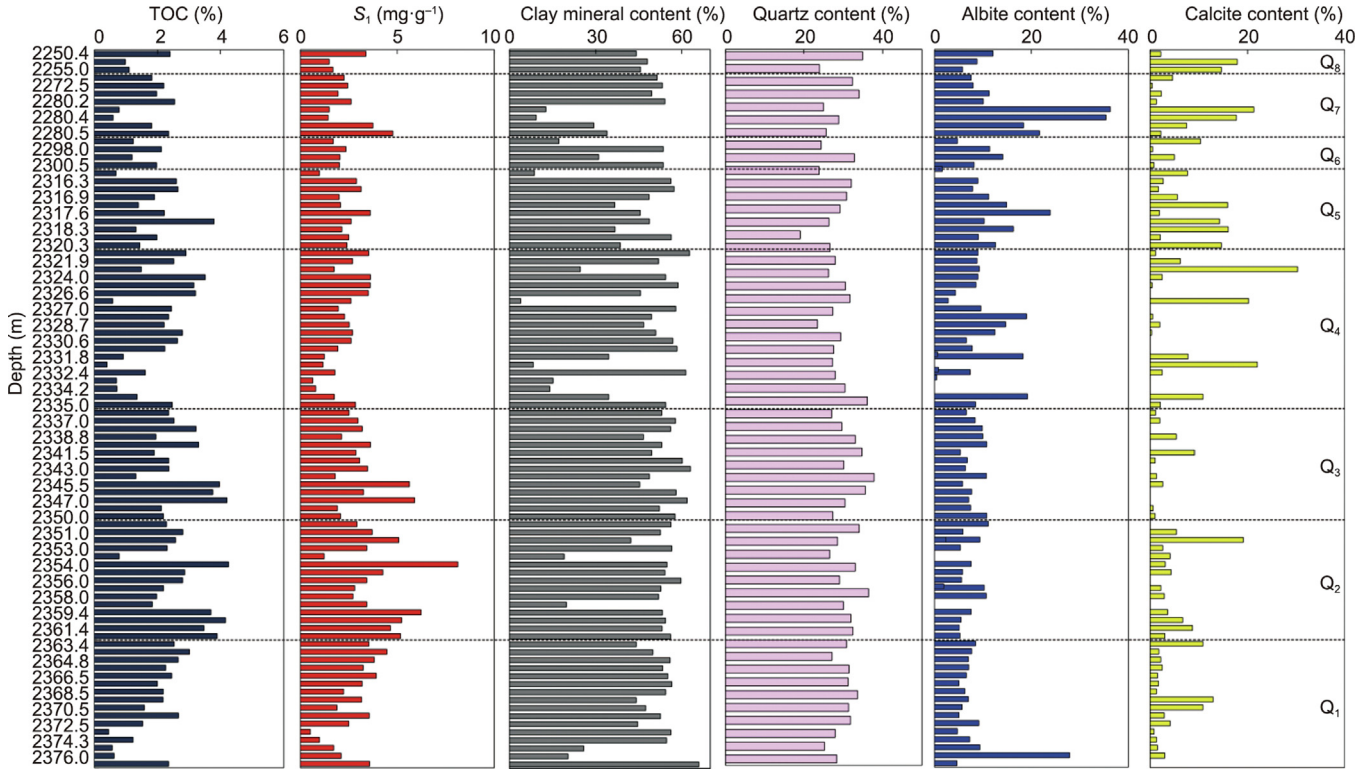

Fig. 2. Mineral composition distribution of the Well Guye 2HC in the Songliao Basin.

largest continental oil field [38,39]. The oil in the Daqing placanticline comes from the depressions on both sides, and the oil of the Putaohua, Gaotaizi, and Fuyu oil layers predominantly comes from the source rocks in the Qingshankou Formation [40].

During the sedimentary period of the Qingshankou Formation, planktonic algae flourished, and the organic matter was mostly layered algae [33–35,37]. Lamalginite in different depressions and sedimentary facies belts accounted for 83%–92%, and terrige-

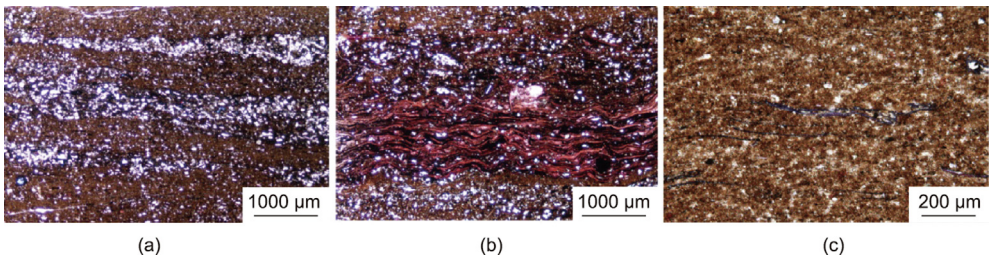

Fig. 3. Shale facies characteristics of the Qingshankou Formation in the Well Guye 2HC. (a) Felsic shale facies, 2492.05 m; (b) mixed shale facies, 2299.3 m; and (c) clay shale facies, 2330.6 m.

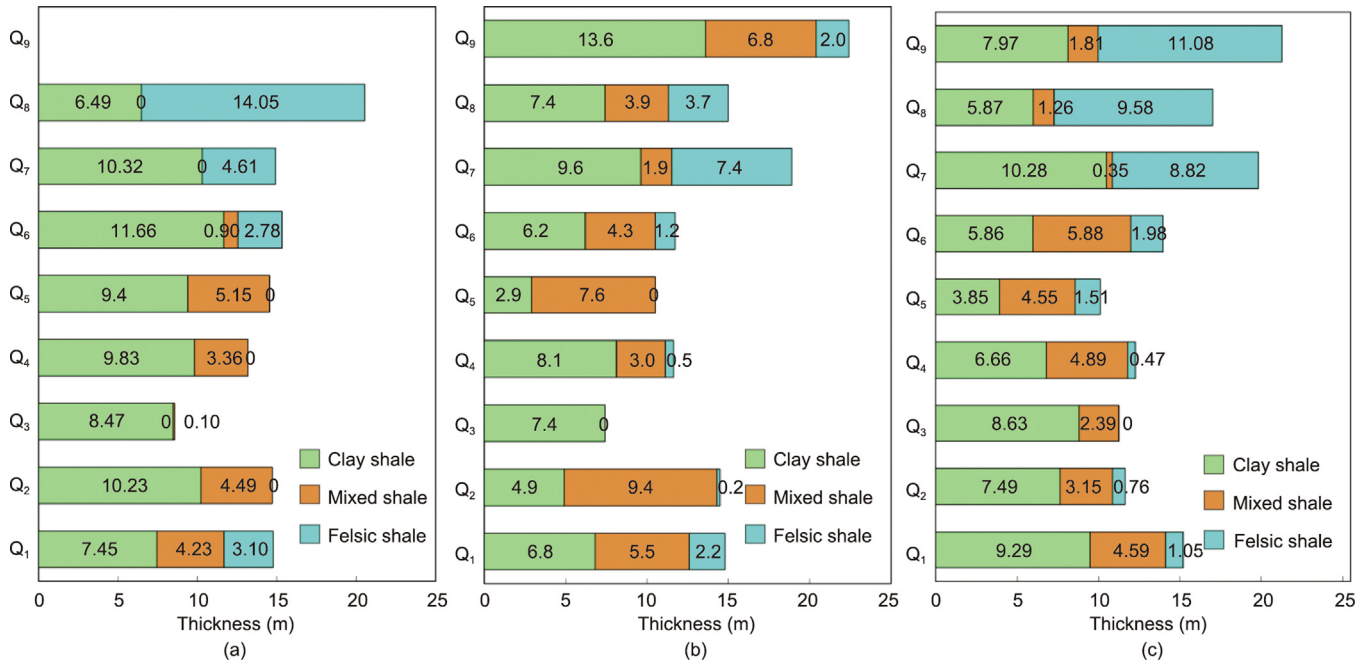

Fig. 4. Vertical variation of the lithofacies of three wells in the Gulong Sag, Songliao Basin. (a) Well Guye 8HC, (b) Well Guye 2HC, and (c) Well Guye 3HC.

nous organic matter was generally less than 10%. The sedimentary environment was generally anaerobic–anoxic, and the organic matter was mainly oil-prone types I and II_1 kerogens. Development of alginite was an important basis for hydrogen accumulation and the high potential for oil generation in Gulong shale. The shale of the Qingshankou Formation has high organic matter abundance. The TOC content is generally 1.50%–2.50%, with an average of 2.20% and individual high values of up to 13.25%. The hydrogen index (HI) value reaches 600–800 $mg{\cdot}g^{-1}$, with an average of 750 $mg{\cdot}g^{-1}$. The HI value of the First Member in the Qingshankou Formation is up to 1000 $mg{\cdot}g^{-1}$, and that of the Second Member is up to 700 $mg{\cdot}g^{-1}$. The hydrocarbon generation conversion rate is up to 78.4%, and the high-quality lacustrine organic matter has excellent oil generation potential. The vitrinite reflectance (R_o) is 0.75%–1.70%, showing medium–high maturity. Chloroform bitumen A is 0.27%–1.32%, with an average of 0.63%. The free hydrocarbon content from rock eval analysis S_1 values representing free hydrocarbons are generally 2–8 $mg{\cdot}g^{-1}$, with an average of 5.31 $mg{\cdot}g^{-1}$. Vertically, the S_1 value of the shale in the lower part of the First Member in the Qingshankou Formation is the highest, generally greater than 8 $mg{\cdot}g^{-1}$, followed by 6 $mg{\cdot}g^{-1}$ in the upper part of the First Member and the Second Member, with a thickness of 100–240 m (Fig. 5). On the plane, the free hydrogen content in the center depression is the highest, gradually decreasing toward the margin.

Within the classic pattern of hydrocarbon generation and the evolution of kerogen established by Tissot and Welte [40], the hydrocarbon generation threshold can be determined from the hydrocarbon generation quantities of different types of organic matter. However, the residual hydrocarbon quantity and hydrocarbon generation evolution in the source rocks have not been further analyzed. Until the discovery of shale oil and gas, more attention was paid to a detailed study of the hydrocarbon expulsion efficiency and the accumulation potential of residual hydrocarbons. Chen et al. [41] believed that the types I and II organic matter in the source rocks are similar in their hydrocarbon expulsion efficiency and expulsion patterns. The relative hydrocarbon expulsion efficiency of the organic matter is less than 45% in the low maturity period, 85%–90% during the peak of oil generation, and up to 90% at the lower limit of the oil generation window. Based on Tissot's hydrocarbon generation and evolution pattern, Zhao et al. [10] established the hydrocarbon generation, expulsion, and retention patterns of organic matter in continental shale. According to this pattern, when R_o is 1.0%–1.6%, large amounts of liquid hydrocarbons are generated; when the R_o value is about 1.0%, the residual hydrocarbon reaches the maximum, accounting for about 25% of the total hydrocarbons generated. When R_o is higher than 1.3%, there is almost no residual liquid hydrocarbon in the shale, which is inconsistent with the current exploration-based understanding of Gulong shale oil.

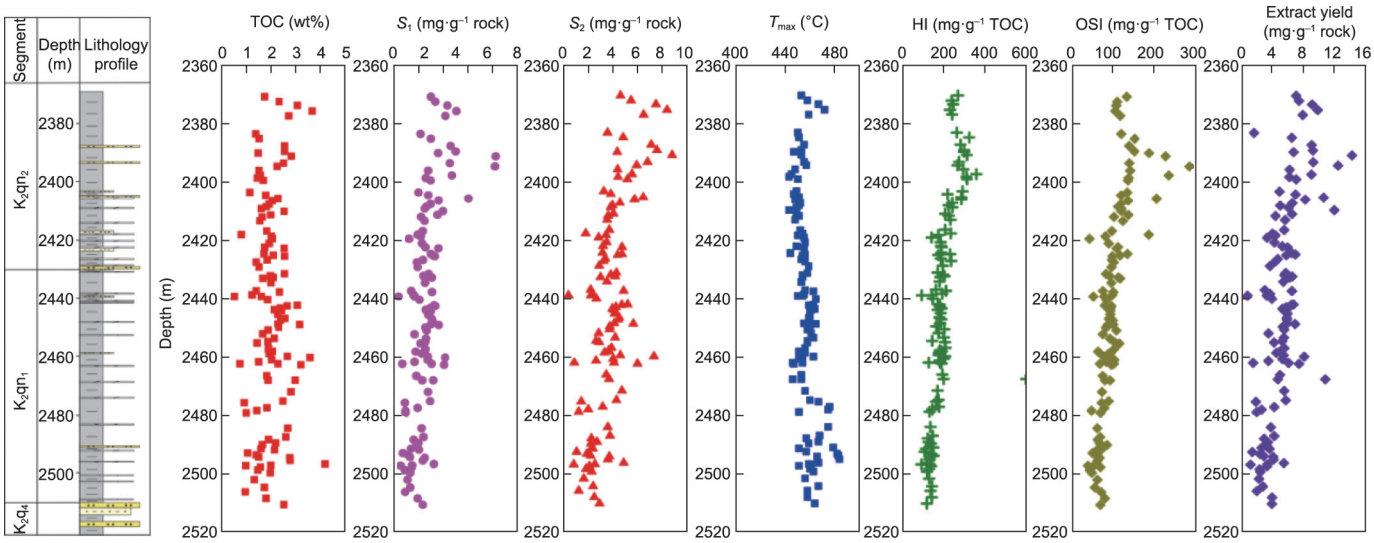

Fig. 5. Comprehensive geochemical evaluation of Well Guye 3HC in the Songliao Basin. S_2: hydrocarbon content of rock eval test during 300–600 °C; K_2: upper Cretaceous; q: Quantou Formation.

The current geothermal gradient of the Qingshankou Formation in the Songliao Basin is 3.5–6.0 °C per 100 m [42], while the paleogeothermal gradient during the Middle and Late Cretaceous was 5.25–6.30 °C per 100 m. Clearly, the paleogeotemperature in the Songliao Basin was higher than the current temperature, and the paleogeothermal gradient in this location is higher than that in other domestic basins. The oil generation threshold of the Songliao Basin is relatively shallow. Early research established that strata in the Songliao Basin with a depth of 1500–2200 m reached the oil generation window (with a corresponding R_o of 0.7%–1.3%) and then entered the condensate and wet gas period [39,40]. However, the lacustrine shale generation period and the oil properties cannot be accurately determined due to the absence of vitrinite and R_o values, as type-I organic matter in the lacustrine environment is rich in alginite. The traditional Easy% R_o index model, which is based on foreign type-III organic matter [43] and the discrete distribution of activation energy, $R_o = e^{-1.6+3.7r}$ (where r represents the conversion rate), is not applicable for the lacustrine hydrogen-rich shale in this study. Therefore, this study established a R_o correction model for Gulong shale (Fig. 6) with a linear model and a new normal activation energy distribution scheme: $R_o = 6.7r + 0.3$. Using the R_o calibration of 32 typical wells, the paleotemperature evolution history of Gulong shale was reconstructed in this study. The Qijia–Gulong Sag had a high paleotemperature and experienced the highest paleogeotemperature in the late sedimentary period of the Minghuazhen Formation, reaching 175 °C. This high paleotemperature field promoted the maturity of the source rocks, resulting in a high hydrocarbon generation conversion rate of the organic matter in Gulong shale. As a result, the main sag entered hydrocarbon generation early, with large quantities of oil generated. The calculated total oil generation quantity of the First Member of the Qingshankou Formation in the north Songliao Basin is 4.48×10^{10} tonnes, including an accumulated oil generation quantity of 1.16×10^{10} tonnes in the late sedimentary period of the Nenjiang Formation and 2.15×10^{10} tonnes in the late sedimentary period of the Sifangtai Formation, which is mainly distributed in the Gulong Sag.

During sample preservation and experimental treatment, light hydrocarbons may be lost. Therefore, based on quantitative nuclear magnetic resonance (NMR) analysis with forward modeling of hydrocarbon generation and expulsion, this study recovered the lost hydrocarbons, corrected the amounts of adsorbed hydrocarbon in low-maturity shale samples of the Qingshankou Formation, and established a calculation model for the hydrocarbon expulsion efficiency of the source rocks in the Qingshankou Formation (Eq. (1)). It is calculated that the hydrocarbon expulsion efficiency in Well Chao 21 is 16.5% when R_o is 0.83%; that in Well Zhao 2911 is 39.0% when R_o is 0.93%; that in Well Guye 36 is 32.0% when R_o is 1.13%; that in Well Ao 34 is 48.0% when R_o is 1.23%; that in Well Guye 2HC is 46.0% when R_o is 1.38%; and that in Well Guye 3HC is 48.0% when R_o is 1.40. These data reveal that at least half of the liquid hydrocarbons remained undischarged after the peak period of oil generation, which is an important basis for shale oil accumulation.

$$\text{EEF} = \frac{\text{hydrocarbon expulsion quantity}}{\text{hydrocarbon generation quantity}} = \frac{\text{HP}_0 - (\text{HP} + L_h)}{\text{HP}_0 - S_2\alpha} \quad (1)$$

where EEF is the hydrocarbon expulsion efficiency (%); HP is the current hydrocarbon generation potential (S_1 + S_2) (mg·g^{-1}); HP_0 is the initial hydrocarbon generation potential (mg·g^{-1}); L_h is the light hydrocarbon loss correction (mg·g^{-1}); S_2 is hydrocarbon content of rock eval test during 300–600 (mg·g^{-1}); and α is the correction coefficient of adsorbed hydrocarbon (0–1), $(S_2 - \triangle S_2)/S_2$.

4. Storage space and physical property

There are many reservoir spaces in Gulong shale oil, which can be characterized into two main types; micro–nano pores and microfractures (lamellar fractures) [30]. The pores include intergranular pores of clastic minerals, intergranular pores of clay minerals, organic matter pores, and dissolution pores (Fig. 7). Analysis of nitrogen adsorption and high-pressure mercury injection shows that the pore diameters are mainly 10–30 nm [3,29]. The intergranular pores of clastic minerals include intergranular pores of clay minerals and intergranular pores formed by quartz, feldspar particles, and other minerals. These pores are residual pores under compaction, with relatively large pore diameters, and are one of the major providers of storage space in Gulong shale reservoirs. The intercrystalline pores of clay minerals are mainly pores formed between illite, kaolinite, and other minerals, as well as pores formed after the dissolution of secondary quartz minerals, feldspar, and calcite. These pores are formed with a small scale, poor connectivity, and strong heterogeneity [44]. The reservoir spaces are mainly pores related to clay minerals, but they cannot form continuous flow channels on a micro-nano scale, as the connectivity of the matrix pore-throat system is poor, with the pore-throat coordination number being less than 0.1. Organic matter pores include

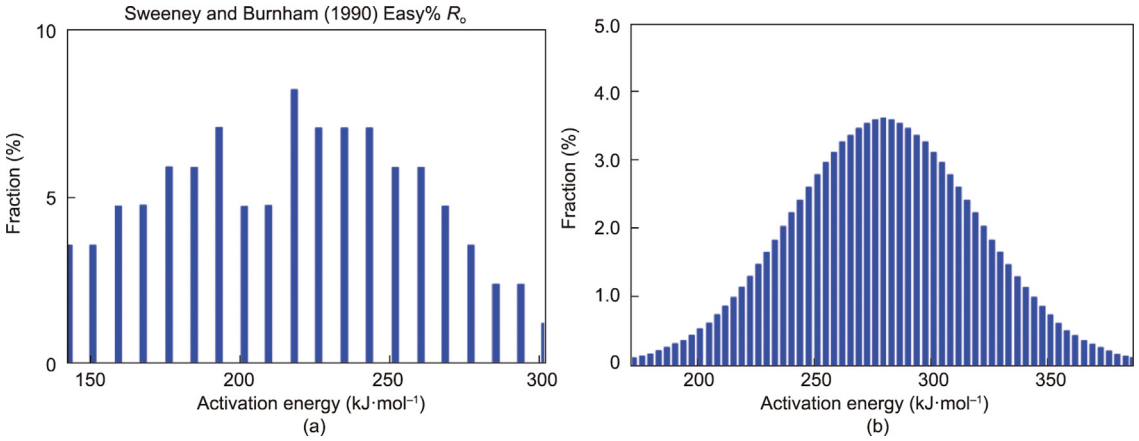

Fig. 6. Activation energy distribution of the vitrinite reaction. (a) Distribution of the activation energy of the Easy% R_o vitrinite reaction; (b) distribution of the activation energy of the Gulong vitrinite reaction.

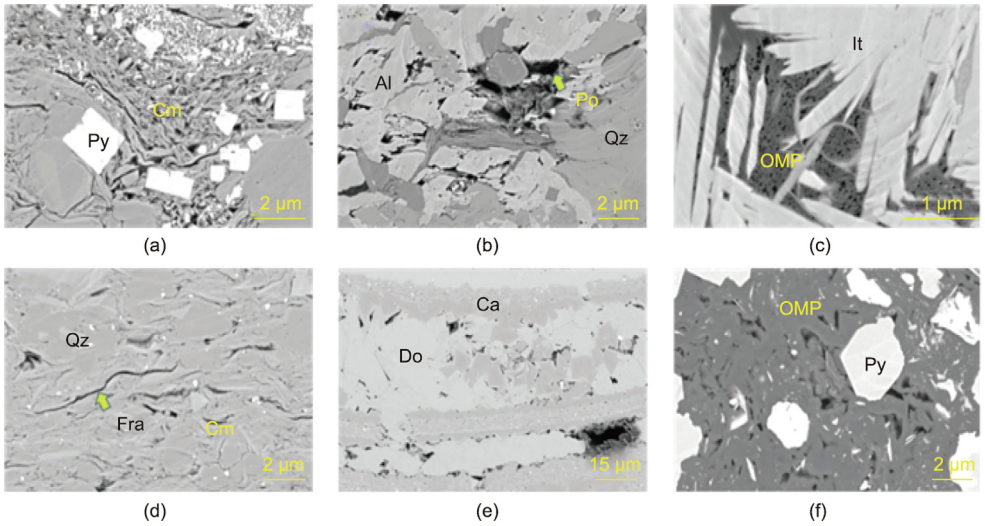

Fig. 7. Typical inorganic pores, fractures, and organic matter pores in Gulong shale. (a) Scanning electron microscope (SEM) image of intra-clay mineral pores, and the clay minerals are dominated by illite; (b) SEM image of inter-granular pores, and the pores are distributed among albites and quartzs; (c) SEM image of organic matter pores and the organic matter is distributed in the illites; (d) SEM image of micro-fractures that are developed in the clay minerals; (e) SEM image of inter-carbonate mineral pores, and obvious oil seepage was observed in the lower right part; (f) SEM image of organic matter pores, and pyrites were observed in the organic matter. The percentage of pore-fracture combinations related to clay minerals, pores related to non-clay minerals, and organic matter pores are 70%, 20%, and 10%, respectively. Py: pyrite; Cm: clay mineral; Po: pore; OMP: organic matter pore; Qz: quartz; Fra: fracture; Do: dolomite; Ca: calcite.

pores formed during the evolution of organic matter [45] and pores developed in the complex of organic matter and clay minerals, which generally have small pore-throats and large quantities. The pores developed in organic matter account for about 10%, while the pores formed in the complex composed of newly discovered organic matter and clay minerals account for about 40%, providing favorable reservoir spaces for Gulong shale. Field emission scanning electron microscope (FE-SEM) statistics show that organic matter pores with diameters less than 10 nm account for 45.3% of the total quantity, and pores with diameters greater than 30 nm account for 97.5% of the total area. The results show that pores with diameters greater than 30 nm play a key role in shale oil storage and recoverability.

The reservoir spaces in Gulong shale are characterized by microfractures, including lamellar fractures, hydrocarbon generation fractures, and diagenetic fractures. Microfractures connecting with pores can form hundreds of millions of fracture-pore reservoirs—not only reservoir spaces but also seepage channels for shale oil development. As mentioned above, Gulong shale has many well-developed millimeter-scale laminar textures. Based on differences in mineral compositions, the textures in Gulong shale can be divided into three types: ostracod-carbonate laminar, felsic silty sand laminar, and clay mineral laminar. These three lamina types are the base for the development of lamellar fractures. Macroscale observation confirms that the density of the lamellar fractures is about 1000–3000 pieces·m^{-1}. In the First Member of the Qingshankou Formation, the density is up to 2000–3000 pieces·m^{-1}, which is the maximum. Based on observation and statistics of the fine core description, the average density of the lamellar fractures in the Q_1–Q_3 oil layers is the highest, close to 2000 pieces·m^{-1}, and the density decreases upward. The average density of the Q_9 oil layer is 800–900 pieces·m^{-1}. Analysis using nitrogen adsorption and high-pressure mercury intrusion shows that the pore diameter is mainly 10–30 nm. The width of the

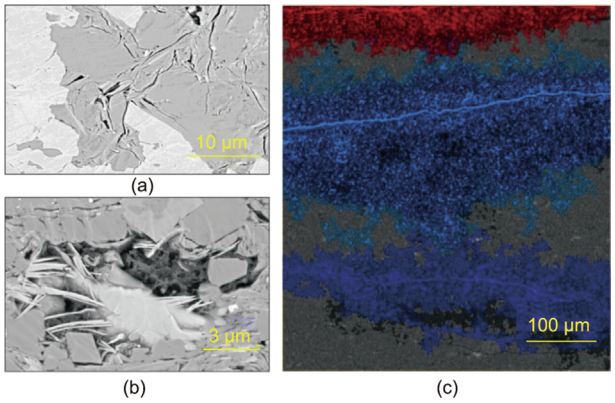

Fig. 8. Pore-fracture texture of (a) 10 μm and (b) 3 μm, and (c) connectivity related to clay minerals in Gulong shale (the different colors in (c) represent different fracture systems).

lamellar fractures is concentrated at 10–40 μm and is up to the millimeter level. The effective porosity is 1.18%, and the contribution rate to the reservoir space is up to 14%. The high-porosity areas are connected with the fractures and extend vertically up to 250 μm. The lamellar fractures and adjacent pores are connected to form fracture-pore reservoirs, which greatly improve the reservoirs' physical properties.

In general, pore-fracture combinations in the matrix of the Gulong shale related to clay minerals comprise the main storage spaces (Figs. 7(a) and (d)), accounting for 70% of the total storage spaces. These pore-fracture combinations can be divided into three types: termination at the end of fracture dislocation, bending and turning of fractures, and grapevine column connections (Fig. 8). These connection methods provide effective space for pure shale reservoirs and favorable seepage channels for shale oil accumulation and high production.

Upon combining simulation experiments of hydrocarbon generation with the physical properties of the shale, it was found that the porosity and permeability of the shale are primarily controlled by the initial organic carbon content. The higher the initial organic carbon content, the larger the porosity and the permeability. With increasing maturity, complex fracture networks form in the shale [46,47]. During different evolution periods, scanning electron microscope (SEM) images of Gulong shale reveal that contraction and hydrocarbon generation from layered algae form organic pores that are distributed along the layers (Fig. 7). This is different from the marine shales in Longmaxi, Sichuan, China, and in North America, which easily form honeycomb-like organic pores. Organic matter pores and fractures increase with increase of R_o and TOC content. When R_o > 1.0%, organic pores and fractures proportion ranges from 10% to 70%. With increasing maturity, the lamellar algae in Gulong shale formed a large number of organic pores and fractures along the layers. Under FE-SEM, it was found that the density of lamellar fractures may exceed 1×10^4 pieces·m^{-1} and that the proportion of organic fractures and pores can reach as high as 68.2%. With an increase in R_o, chlorite flake aggregates form around the organic clay complex, with the pores being supported by the angular chlorite flakes. Authigenic quartz can develop in the pores, which improves the reservoir's properties and brittleness.

The reservoir properties differ in the different layers of Gulong shale. The measured porosity of a core tested using helium is about 8.4%–9.1%, and the differences between the oil layers are small. The effective porosities of the Q_8 and Q_9 oil layers are high. Field full-diameter two-dimensional (2D) NMR evaluation technology was used to measure the core in real time when it was out of the well. The effective porosity is 6%–8%, and the total porosity is 16%–18%, which is 3% higher than the laboratory results. Under overpressure formation conditions, the underground porosity should be higher than that measured under surface experimental conditions, and the reservoir properties are also improved. The horizontal permeability of the shale measured by a surface gas test is generally 1.00×10^{-5}–5.00×10^{-4} μm^2, and the vertical permeability is generally 1.00×10^{-6}–5.00×10^{-5} μm^2. The horizontal permeability is normally about ten times the vertical permeability. Vertically, there is no clear distinction between each oil layer's permeability. The permeabilities of the Q_5–Q_7 oil layers are relatively high. The horizontal permeability is higher than 1.00×10^{-4} μm^2, and the vertical permeability is higher than 1.00×10^{-5} μm^2. Vertically, the Q_1–Q_4 layers are mainly composed of organic pores and fractures, while the Q_5–Q_9 layers are mainly composed of organic and non-organic pores and fractures. Nitrogen adsorption and mercury injection experiments show that the porosity of clay shale is the highest, at about 7%–9%, which is higher than that of siltstone and shell limestone.

It is worth mentioning that the formation porosity under overpressure is 5.5%–28.1%, which is higher than that under normal fluid pressure. With the increase of pore pressure, the measured value of shale porosity increases gradually. Under overpressure conditions (i.e., a pore fluid pressure of 45 MPa and a pressure coefficient of 1.7), compared with the normal pressure of 25 MPa, the porosity of the sample from Well Guye 7 increases by 13.5%–28.1%, with an average of 22.4%, while the porosity of the sample from Well Guye 8 increases by 5.5%–9.5%, with an average of 7.6%.

Oil generation, pore formation, mineral transformation, corrosion transformation, and overpressure in Gulong shale are correlated, which controls the target layers and the accumulation areas of the shale oil. Pore evolution correlates well with the thermal evolution of organic matter and minerals.

5. The shale oil accumulation mechanism

Research on conventional oil and gas accumulation in the Songliao Basin confirms that, after entering the oil generation window, the source rocks in the First Member of the Qingshankou Formation discharged hydrocarbons upward into the middle oil-bearing assemblage, including the Saertu, Putaohua, and Gaotaizi oil layers, and discharged hydrocarbons downward into the lower oil-bearing assemblage, including the Fuyu and Yangdachengzi oil layers [38–40]. Oil and gas accumulation in the Qijia–Gulong Sag can be divided into three periods: The first period is the late sedimentary period of the Nenjiang Formation; the second period is the end of the Cretaceous (the sedimentary period of the Sifangtai–Mingshui Formations); and the third period is the end of the Paleogene. On the plane, the oil and gas generated in the Qijia–Gulong Sag migrated eastward under the action of fluid potential, to the Daqing placanticline [40]. Based on geochemical analysis of the crude oil, we found that the terpane content of the oil in the Daqing placanticline is 50–900 μg·g^{-1}, the sterane content is 40–110 μg·g^{-1}, and the triarylsterane content is 0.37–6.97 μg·g^{-1}, which is the same as source rocks with an R_o of 0.8%–1.0%. It is therefore considered that the oil in the First Member of the Qingshankou Formation of the Daqing placanticline was produced during an evolution period when the R_o was 0.8%–1.0%. Analysis of inclusion accumulations also proves that Gulong shale oil was generated at the same time as the late self-sealing of the shale. One phase of oil inclusions with blue fluorescence occurs in the calcite vein of Well Guye 8HC in the First Member in the Qingshankou Formation, reflecting the light quality of the oil. The main peak of homogenization temperature of the associated brine inclusions is 130–150 °C. Combining the burial

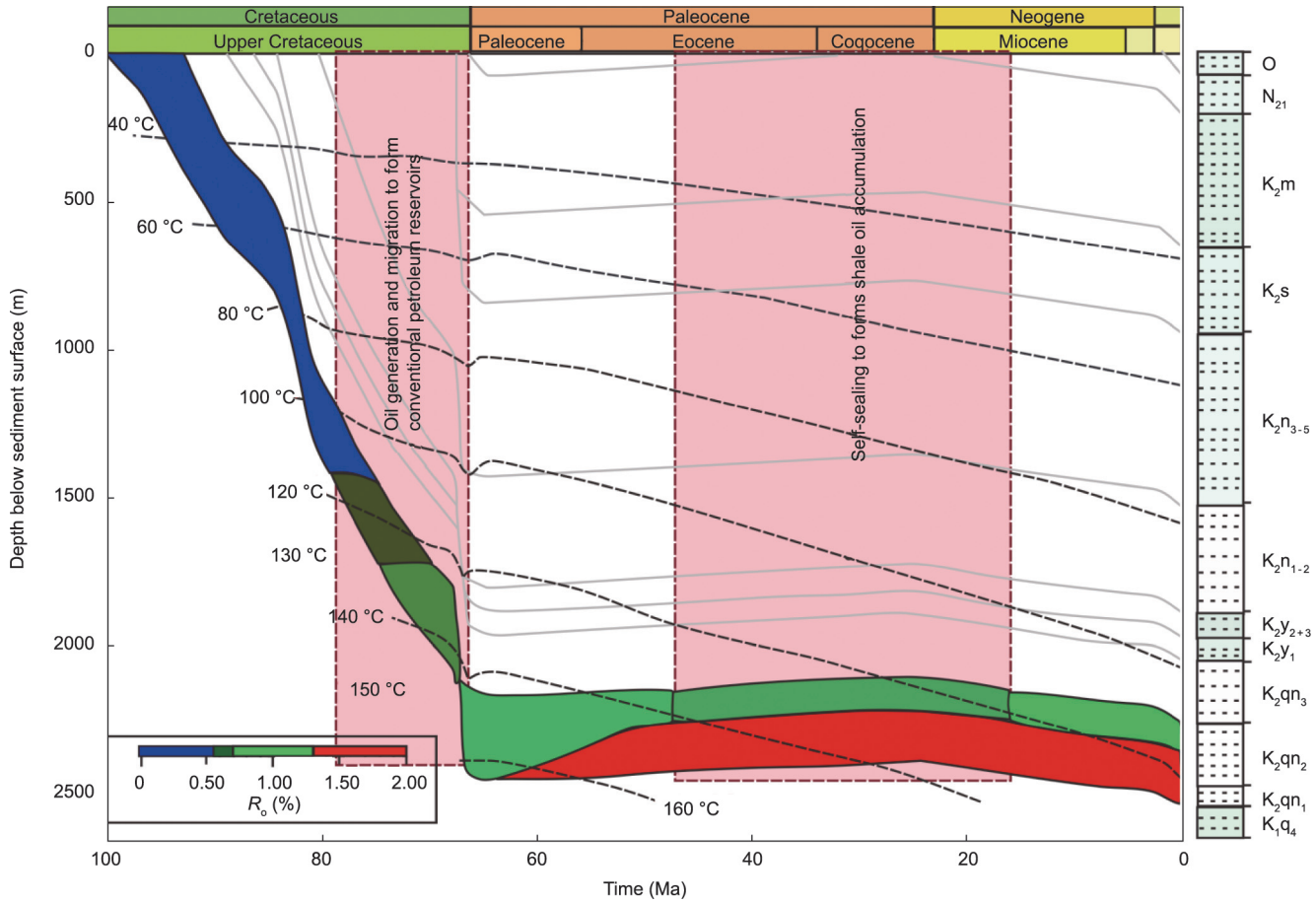

Fig. 9. Burial and thermal history of Well Guye 8HC.

and thermal histories reveals that the inclusions formed in the sedimentary period of the Yi'an Formation and reflect the late self-sealing of the shale oil (48–18 Ma) (Fig. 9). The self-sealing and accumulation of oil and gas may be the result [48] of the *in situ* preservation of oil and gas molecules under overpressure [29]. The overpressure may have been generated by blocked outflows of oil and gas and the blocked entrance of external fluid when the capillary pressure and the adsorption force on the fluid are greater than the buoyancy, which might have been caused by the reservoirs' tightness as thermal evolution progressed.

Based on the geochemical characteristics, the Q_1–Q_9 oil layers from the First to the Second Members of the Qingshankou Formation in Gulong Sag can be divided into four sections: Q_9, Q_8–Q_7, Q_6–Q_5, and Q_4–Q_1. The oil and gas characteristics of these four sections vary noticeably, and the methane carbon isotope levels of the mud gas imply segmentation and abrupt interfaces. With an increase in depth, the TOC changes little, T_{max} increases, and the HI decreases, indicating that the maturity gradually increases going downward. Isotope analysis of the group components in the extractives shows that the saturated hydrocarbon content increases gradually in the Q_9 layer, decreases in the Q_8–Q_7 layers, increases again in the Q_6–Q_5 layers, and decreases slightly in the Q_4–Q_1 layers, while the isotopic evolution of components is just the opposite. The aromatic hydrocarbon content shows the opposite trend, but its component isotope evolution is consistent. Abrupt changes in shale oil properties and isotopes occur at the key lithofacies interfaces and lithology interfaces, and the lithology interfaces often correspond with the calcite cemented tight sandstone or carbonate strata.

There are clear differences in oil composition, Pr/nC_{17} and Ph/nC_{18} values, and carbon isotope differences between non-hydrocarbon asphaltene and saturated hydrocarbon in different layers of Gulong shale. Gulong shale oil evolved segmentally (Fig. 10), controlled by the hydrocarbon migration and accumulation process or the differences between initial kerogen types. Migration within the shale oil layers of Q_1–Q_9 may also explain the differences in oil and gas properties in different layers.

6. Rock mechanics and fracability

On the microscale, the lamellar and laminar textures of Gulong shale are developed, and the rock mechanical properties and fracturing mechanism are complex. Gulong shale has a high clay mineral content and strong diagenesis, showing characteristics of high hardness, a high elastic modulus, and high fracture toughness. In addition, both the interlayer hardness ratio and the resistance to fracture propagation through the layers are high. The content of brittle minerals in the shale is relatively stable, and the content of quartz is 25%–35%. The mechanical properties and fracture mechanism of the laminar shale are different from those of the pure shale. The laminar shale is composed of large dispersed particles, while the pure shale is composed of small particles mixed with clay. Based on a microscale hydraulic fracturing numerical model reconstructed from digital cores, we discovered that lamellar textures can prevent the vertical extension of hydraulic fractures, and that penetration of the fractures is controlled by *in situ* stress, drainage, and fracturing fluid viscosity. Physical simulation

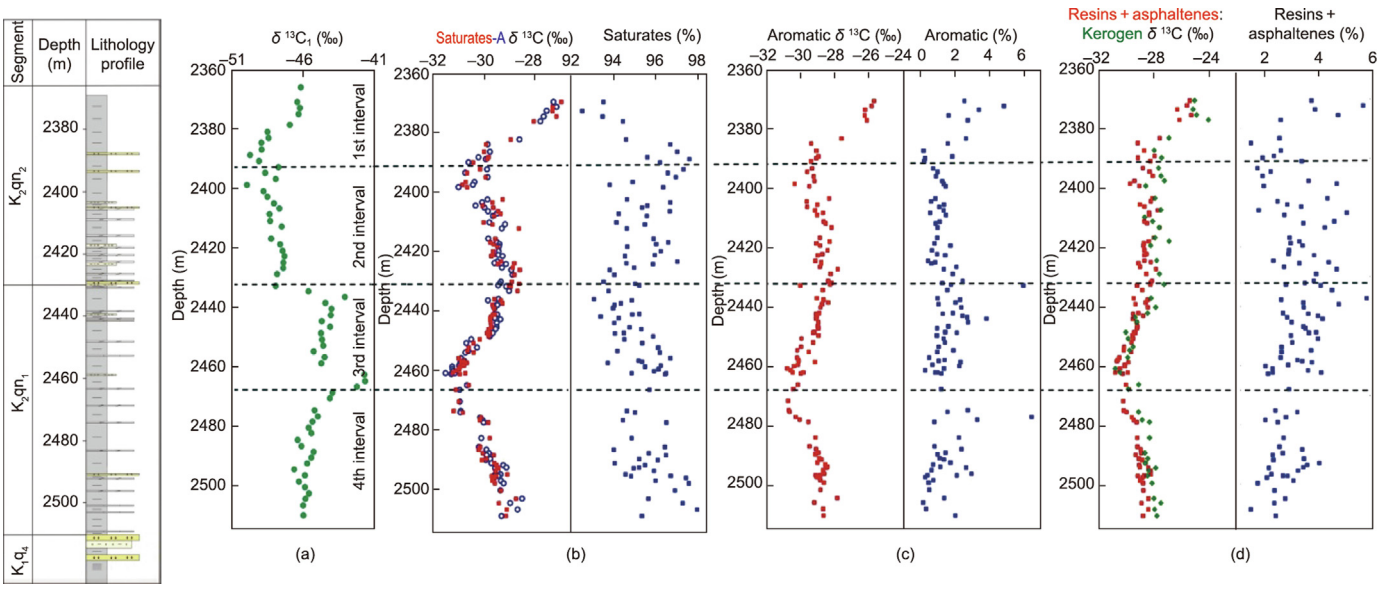

Fig. 10. Isotopic evolution of group components in extracts from Well Guye 3HC.

tests of hydraulic fracturing with similar materials show that, with an increase in the lamellar angle, the fracture initiation pressure decreases, the lamellar texture becomes easier to open, the fracture geometries tend to be more complex, and major vertical fractures are not observed near the wellbore.

Reconfigured by *in situ* stress, Gulong shale shows increased strength and stronger plastic characteristics. Compared with laminar shale, pure shale samples are more significantly affected by restoration and reconfiguration by *in situ* stress. At high temperatures, the influence of lamellar textures on fracture extension is more significant. As a result, major fractures are not obvious. The peak load is significantly increased, the elastic modulus is increased, the fracture toughness is increased, and the rate of fracture opening is reduced, indicating stronger plasticity of the rocks under high temperatures and more difficult fracture initiation. Based on these characteristics, a "multilayer pancake" semi-analytical fracture height growth model (FRACMI) is established for Gulong shale. The shear-slip mechanism of Gulong shale can be characterized by splitting the fracture width into two parts: a non-slip component and a bedding-slip disturbance component, which effectively characterizes the shear-slip mechanism related to the bedding interaction. The bedding density can reach 10–20 pieces·m^{-1}.

7. Discussion

7.1. Oil occurrence in different types of shales

The oil in the Songliao Basin generally has a density of 0.6947–0.9804 g·cm^{-3} and is primarily medium oil with a density of 0.85–0.90 g·cm^{-3}. The oil-producing layers mostly occur in the Saertu, Putaohua, and Gaotaizi oil layers of the Daqing placanticline; the Fuyu and Yangdachengzi oil layers in the east of the Daqing placanticline; and the Heidimiao, Saertu, and Gaotaizi oil layers in the west of the Daqing placanticline. Light oil with a density of 0.805–0.850 g·cm^{-3} is mainly found in the western slope area, the Qijia–Gulong Sag, the Daqing placanticline, the Sanzhao Sag, and the Chaoyanggou Terrace. Volatile oil with a density of 0.75–0.80 g·cm^{-3} is found in the Putaohua oil layer of the Qijia–Gulong Sag and in the Yufu and Yangdachengzi oil layers in the Sanzhao Sag [29]. The surface density of Gulong shale oil is generally less than 0.84 g·cm^{-3}. For example, the oil density in the Q_2 oil layer of Well Guyeyouping 1 is 0.798 g·cm^{-3}; in the Q_2 oil layer of Well Guye 2HC, it is 0.782 g·cm^{-3}; in the Q_2 oil layer of Well Songyeyou 1HF, it is 0.837 g·cm^{-3}; and in Well Yingye 1H, it is 0.820 g·cm^{-3}. Formation crude oil generally has a viscosity of less than 0.8 mPa·s, a gas–oil ratio of 70–800, an average content of saturated hydrocarbon of 84.2%, and low contents of aromatic hydrocarbons, non-hydrocarbons, and asphaltene.

The occurrence spaces of Gulong shale oil indicate that all kinds of lithologies and pores contain oil. Organic matter generates hydrocarbons *in situ*, and oil and gas occur *in situ*. Oil is found in 9 nm pores, and lamellar fractures are rich in oil. According to microscopic observation using environmental scanning electron microscope (ESEM), crude oil in the shale occurs in intergranular pores and intercrystalline pores as free oil film and occurs in clay contraction fractures in an adsorption state [49]. Large amounts of spilled crude oil can be observed under FE-SEM, indicating large oil-bearing areas and good oil-bearing properties. The dolomite and siltstone interlayers are relatively tight, with poor porosity and oil-bearing properties. We characterized the oil-occurrence pore diameters in different lithofacies, with the results showing that the major pore space of the clay shale oil is 26–80 nm, the major pore space of the felsic shale oil is 40–80 nm, and the major pore space of the mixed shale oil is 40–80 nm. The oil-occurrence pore diameters in different lithofacies differ. More than 90% of the hydrocarbons in Gulong shale are weak-polar hydrocarbons, and light volatile hydrocarbons occupy most of the pore spaces, while weak-polar macromolecular hydrocarbons occupy pores with diameters less than 32 nm and greater than 64 nm.

The characteristics of pore spaces occupied by different fluids can be revealed by combining a series of oil washing and nitrogen adsorption experiments based on different reagents such as *n*-hexane and dichloromethane [50–53]. The clay shale is composed of large-diameter pores and large amounts of saturated hydrocarbon, and clay shale oil mainly occurs in pores with diameters less than 32 nm. Mixed shale is formed with medium-diameter pores and medium saturated hydrocarbons, and mixed shale oil mainly occurs in pores with diameters less than 8 nm and greater than 64 nm. Felsic shale is formed with small-diameter pores and small amounts of saturated hydrocarbon. Felsic shale oil mainly occurs in pores larger than 64 nm and in a small number of pores smaller than 8 nm. The oil saturation of the First Member of the

Qingshankou Formation, as measured by fluid adduction, is 35%–55%, with an average of 47%. The oil saturation measured by various NMR methods is typically 55%–60%, with a maximum of more than 70%. The movable oil saturation characterized by the nuclear magnetic method is generally 30%–45%.

Multi-channel laser confocal fluorescence analysis shows that there are also differences in the occurrence locations of light and heavy hydrocarbons in the shale layers with different lithologies and depths in a single well. An analysis of 38 samples from Well Guye 8HC found that the shale is generally oil-bearing, but the contents of light and heavy hydrocarbons in different lithologies differ. In clay shale at a depth of 2369.6 m, light hydrocarbons account for 8.21% and heavy hydrocarbons account for 8.42%, with a ratio of light to heavy hydrocarbons of 0.98. The distribution of light and heavy hydrocarbons is relatively uniform. In mixed shale at a depth of 2421.1 m, light hydrocarbons account for 9.21% and heavy hydrocarbons account for 6.99%, with a ratio of 1.32. There is little differentiation between light and heavy hydrocarbons (Fig. 11). The distribution of light and heavy hydrocarbons in the felsic shale is affected by the quantity of organic matter. In felsic shale with low TOC contents, the organic matter abundance is 0.868%, light hydrocarbons account for 3.48%, heavy hydrocarbons account for 0.35%, and the ratio of light to heavy hydrocarbons is 9.94. There is obvious differentiation between light and heavy hydrocarbons. In felsic shale with a high TOC content, the organic matter abundance is 3.74%, light hydrocarbons account for 14.00%, and heavy hydrocarbons account for 13.99%, so the ratio of light to heavy hydrocarbons is 1. The distribution of light and heavy hydrocarbons is relatively uniform. Clearly, the micro-distribution of light and heavy hydrocarbons is affected by maturity and burial time. Mixed shale and clay shale with high TOC contents have similar contents of light and heavy hydrocarbons. Felsic shale with many sandy laminae and a low TOC content contain a large amount of light and small amounts of heavy hydrocarbons.

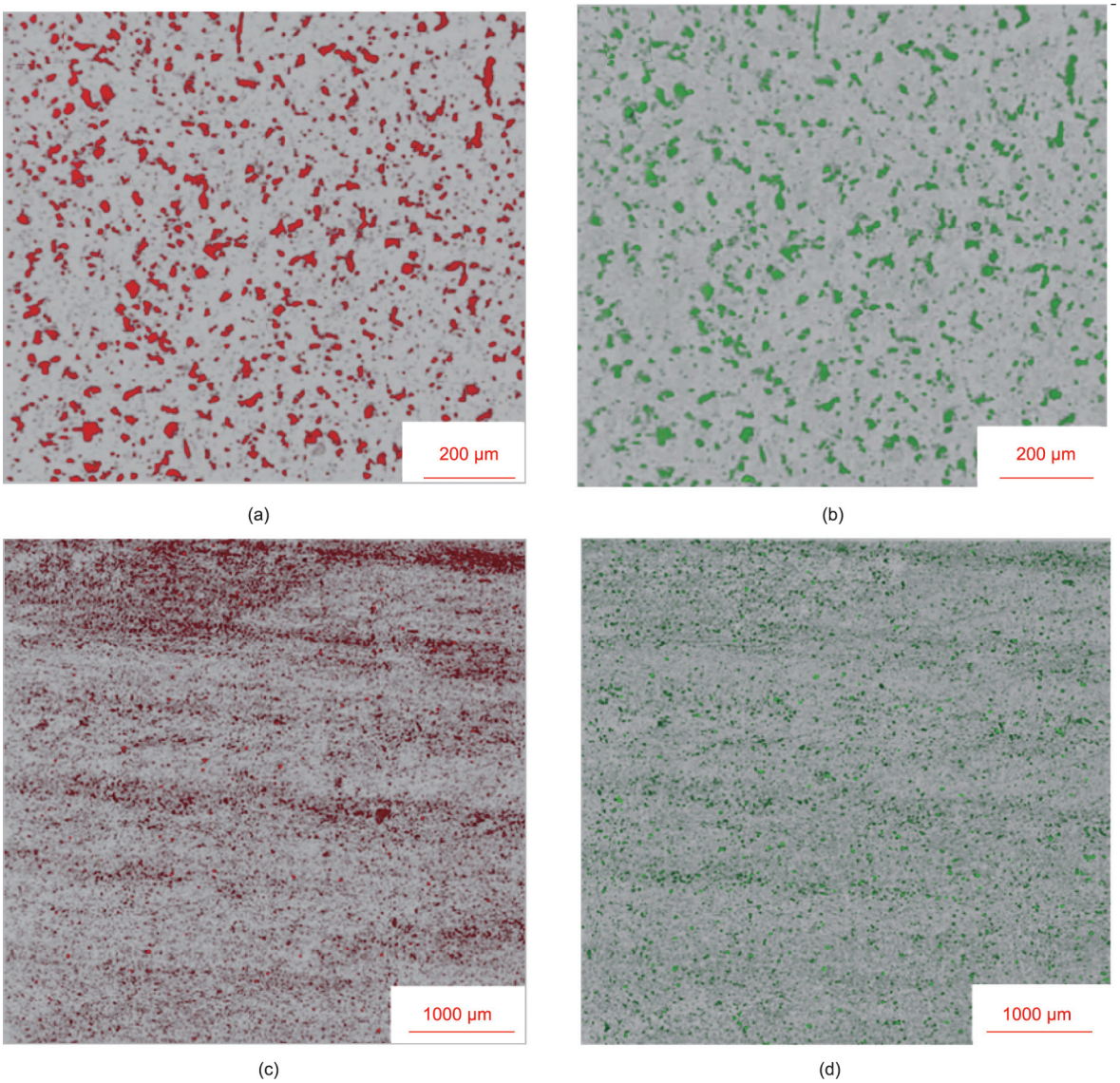

Fig. 11. Micro-distribution of oil and gas in samples from different layers of Well Guye 8HC. (a) Light hydrocarbon; (b) heavy hydrocarbon in clay shale at the depth of 2369.6 m, where light hydrocarbon accounts for 8.21%, heavy hydrocarbon accounts for 8.42%, and the light-heavy hydrocarbon ratio is 0.98; (c) light hydrocarbon; and (d) heavy hydrocarbon in mixed shale at the depth of 2421.1 m, where light hydrocarbon accounts for 9.21%, heavy hydrocarbon accounts for 6.99%, and the light-heavy hydrocarbon ratio is 1.32. The classification of light and heavy hydrocarbons is based on the laser length, and the wavelength used to classify light and heavy hydrocarbons are 405 and 480 nm, respectively.

7.2. The relationship between movable fluid saturation and shale

Gulong shale oil has high thermal maturity and good fluidity. With a high degree of thermal evolution, large amounts of oil and gas are generated with light weight, and the gas–oil ratio increases to 70–800 $m^3 \cdot m^{-3}$, or even up to 2000 $m^3 \cdot m^{-3}$. After 72 h of continuous extraction with dichloromethane, the results show that Gulong shale has a high conversion rate and is generally oil-bearing. The S_1 values of the shale show weak-polar hydrocarbons, and about 80% of the S_2 value also shows generated heavy hydrocarbons. The charging effect observed under an electron microscope shows largely lost mobile oil, while some heavy hydrocarbons are almost immobile, displaying adsorption and having the negative effect of blocking pore-throats. Samples with relatively high TOC values contain more volatile hydrocarbons. Weak-polar hydrocarbons and volatile hydrocarbons occupy most of the pore spaces. The heavy-polar hydrocarbons also increase, and it is difficult for oil flow to occur. As a result, the porosity of the reservoir is reduced due to adsorption and blockage.

High-speed centrifugation and NMR experiments were carried out, and it was found that, when the centrifugal force is 2.6 MPa, the total movable oil ratio is 8.66%–26.22%, with an average of 13.15%. Nanoscale and microscale movable oils are the principal components, accounting for 36.11% and 40.63%, respectively. Almost all saturated oils in lamellar fractures, microfractures, and other areas are movable oil. TOC and lithofacies control the mobility of Gulong shale oil. When the TOC is 1%–3%, it is not easy to block pore-throats with large diameters, high hydrocarbon contents, and medium-polar hydrocarbon content. As a result, clay shale and mixed shale have the best oil content and mobility. Clay shale with a TOC greater than 3% has a high hydrocarbon content, but high-polar hydrocarbons may lead to pore-throat blockage and poor mobility. Felsic shale with a TOC less than 1% has a low hydrocarbon content and small quantities of movable oil. The proportion of movable oil controlled by the large throat of laminated felsic shale is greater than that of clay shale, and more oil can be produced under a small production pressure difference. The higher the clay content, the less the movable oil, the larger the average pore size, and the more movable the oil.

High-pressure physical property analysis of formation fluid samples shows that, in areas with an R_o less than 1.4%, the Gulong shale reservoir can be described as a single reservoir in a critical state (gas–liquid two-phase). High-pressure mercury injection shows that the Gulong shale pores are mainly nano pore-throats. Due to a reduction in pore sizes, more gas components are dissolved in the liquid phase, and the fluid gradually changes from oil-gas two-phase to a single-phase fluid. Due to the space confinement effect on the nano-pores, the critical temperature and pressure of the fluid are lower than those of the bulk fluid. The nano-pore fluid diagram is flatter than the bulk fluid diagram, while the critical point of the nano-pore fluid diagram is lower than that of the bulk fluid diagram.

Inorganic minerals are mostly water-wet, while organic pores are oil-wet. The inorganic pore size is relatively large, and the surface energy of the oil is greater than that of water. Oil can enter both the organic and inorganic pores, while water can only enter the inorganic water-wet pores. The flow caused by molecular movement and wall scattering in organic pores conforms to the Knudsen diffusion principle. When the effective stress exceeds the threshold, the oil in the organic matter is squeezed out, and the pore pressure decreases. Diffusion and imbibition mainly occur in the inorganic pores. As a result, the fluid flows, the pressure in the pores decreases, and the effective stress increases. The fluid in the organic matter is attracted by the organic matter molecules and has no flow. When the organic matter is squeezed and shrunk by inorganic matter, the pore pressure and effective stress increase.

Free oil in the inorganic pores accounts for 40.0%–85.0% and decreases with an increase in the TOC content. The average percentage of organic pores is 20.19%, free oil accounts for 62.0%–85.0%, and adsorbed miscible oil accounts for 8.5%–37.8%. The higher the TOC, the more oil is in an adsorbed miscible state and contained in the organic matter.

The interaction between fluids and pore walls means that the fluid and bulk fluid properties—such as the critical pressure, temperature, viscosity, and interfacial tension—in confined nano-spaces are quite different. In the nano-porosity oil and gas migration model of the shale reservoir (Fig. 12), the adsorbed phase on the pore wall migrates through adsorption and saltation. The free components near the pore wall migrate by adsorption and dissociation. The free components in the middle parts of the pores are not affected by adsorption. Based on the Young–Laplace equation (Eq. (2)), Peng–Robinson equation of state (PR-EOS, Eq (3)), as well as the van der Waals equation of state and the Wilson equation (Eq. (4)), the Research Institute of the Daqing Oilfield Exploration and Development established critical property relationships for fluids in pores of different sizes. Due to the nano-pore confinement effect, the critical temperature and pressure of the fluids in the pores are lower than those of the bulk fluid, and the phase diagram of the pore fluids shows flatter characteristics and lower critical points than that of the bulk fluid. Based on the relationship between critical properties and the bulk-phase fluid component model in Well Guyeyouping 1, with a gas–oil ratio of 500 $m^3 \cdot m^{-3}$, we calculated the critical properties of each component in the confined space fluid with a pore size of 3.5, 10.0, 20.0, and 50.0 nm respectively, and drew corresponding pressure–temperature (P–T) phase diagrams (Fig. 13). With decreasing pore diameters, the critical pressure and critical temperature of the pores also decreased, with the critical properties in pores below

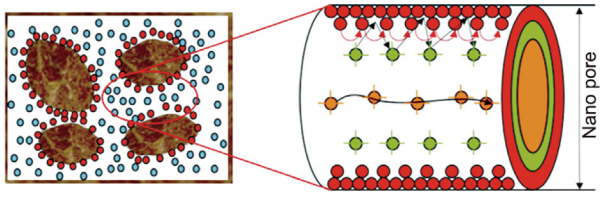

Fig. 12. An oil and gas migration model in a shale reservoir with nano-pores. Blue: water; red: adsorbed phase; green: dissociated phase; orange: free phase.

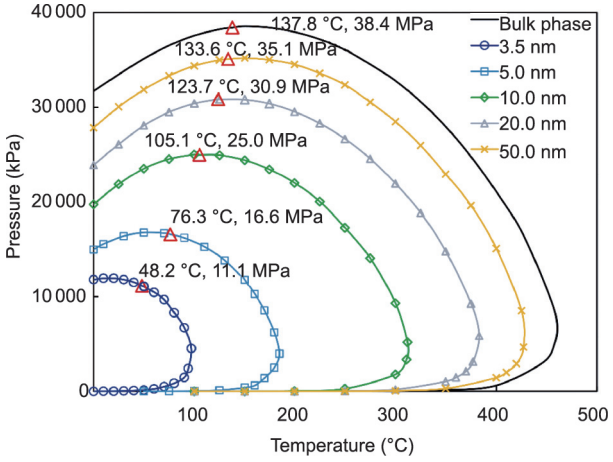

Fig. 13. Pressure–temperature (P–T) phase diagram of fluids with different pore sizes and diameters in Well Guyeyouping 1 with a gas–oil ratio of 500 $m^3 \cdot m^{-3}$.

5 nm decreasing significantly (Eqs. (4) and (5)). The confinement effect delayed the initiation of two-phase flow and decreased the fluid viscosity in the nano-pores. Compared with the bulk fluid model, the oil and gas production stability of the model including nano-pores is stronger.

$$\text{Young—Laplace equation: } P_{\text{cap}} = \frac{2\gamma}{r_{\text{e}}}\cos\theta \tag{2}$$

$$\text{PR–EOS equation: } P = \frac{RT}{v-b} - \frac{\alpha}{v(v+b)+b(v-b)} \tag{3}$$

$$\text{Wilson equation: } K_i = \frac{P_{ci}}{P}\exp\left[5.37(1+\omega_i)\left(1-\frac{T_{ci}}{T}\right)\right] \tag{4}$$

$$\text{Critical temperature correlation: } T_{\text{cp}} = T_{\text{cb}}\left(1-1.1\left(\frac{D}{\sigma}\right)^{-1.353}\right) \tag{5}$$

$$\text{Critical pressure correlation: } P_{\text{cp}} = P_{\text{cb}}\left(1-0.686\left(\frac{D}{\sigma}\right)^{-0.6}\right) \tag{6}$$

where, P_{cap} is the capillary pressure; γ is the interface tension, θ is the contact angle of the vapor–liquid interface with respect to the pore surface; r_{e} is the effective pore radius; P is the system pressure; R is the gas constant, which equals 8.314 J·(mol·K)$^{-1}$; T is the system temperature; α and b are EOS constants; v is the molar volume; T_{c} is the critical temperature; P_{c} is the critical pressure; i represents the physical parameters of component; ω is the acentric factor; T_{cb} is the bulk critical temperature; P_{cb} is the bulk critical pressure; T_{cp} is the critical temperature in pore scale; P_{cp} is the critical pressure in pore scale; D is the pore diameter, and σ is the Lennard–Jones size parameter.

8. Conclusions

The Gulong shale oil reservoir is primarily composed of clay minerals, which distinguishes it from other shale oil reservoirs at home and abroad. Industrial oil production from Gulong shale is a complex scientific process involving sedimentology, geochemistry, rock mechanics, seepage force, surface mechanics, and mechanics. By studying the factors of hydrocarbon retention, occurrence state, and reservoir space, this study reveals a geological frontier of shale from oil generation to oil production that has enormous scientific importance. Following pilot production, the oil recovery and cumulative oil production of single wells in the Gulong Sag can be effectively improved through progress in theories and technologies. The main findings of this work are as follows:

(1) The clay-grade particles of Gulong shale are less than 0.0039 mm, and the clay mineral content is more than 35%;

(2) Gulong shale is characterized by high-quality organic matter, high maturity, and high residual hydrocarbon content;

(3) The favorable reservoir spaces in Gulong shale are the fracture-pore reservoirs composed of pores and the lamellar fractures developed between organic matter and clay mineral complexes;

(4) Gulong shale oil accumulation was formed by late self-sealing;

(5) Clay shale has good oiliness, and its oil occurs in small pores, while felsic shale oil occurs in large pores;

(6) There is higher saturation of movable fluid in the laminar shale;

(7) Gulong shale is characterized by high hardness, a high elastic modulus, and high fracture toughness.

In addition, great improvements have been made in economic development of Gulong shale oil due to the substantial cost reductions achieved by the implementation of advanced engineering technologies and good management. The exploration and development of Gulong shale oil have broad prospects and hold great strategic significance for supporting the sustainable development of the Daqing Oilfield and realizing the continental shale oil revolution in China.

Acknowledgments

This study is supported by the National Natural Science Foundation of China (72088101 and 42090025) and the China National Petroleum Corporation (2019E-26 and YGJ2020-3). We thank Professor Xinhua Ma, Professor Dongbo He, Professor Hong Cao, Professor Lianhua Hou, Professor Xiaomei Wang, Dr. Huajian Wang, Dr. Chang Liu, Dr. Siwei Meng, Ms. Xiaohua Jiang, Dr. Jingya Zhang, Dr. Tianshu Zhang, Dr. Yicai, Dr. Yuhui Huangfu from RIPED, and PetroChina for their support and scientific contribution to this study. We also thank Mr. Jinyou Zhang and Mr. Dongxu He from Daqing Oilfield for their work. We thank CNPC for their permission to publish this paper.

Compliance with ethics guidelines

Wenyuan He, Rukai Zhu, Baowen Cui, Shuichang Zhang, Qian Meng, Bin Bai, Zihui Feng, Zhengdong Lei, Songtao Wu, Kun He, He Liu, and Longde Sun declare that they have no conflict of interest or financial conflicts to disclose.

References

[1] Pan CH. Geological notes: non-marine origin of petroleum in north Shensi, and the Cretaceous of Szechuan, China. China AAPG Bull 1941;25:2058–68.
[2] Sun LD. Gulong shale oil (preface). Pet Geol Oilfield Dev Daqing 2020;39(3):1–7. Chinese.
[3] Sun LD, Liu H, He WY, Li GX, Zhang SC, Zhu RK, et al. An analysis of major scientific problems and research paths of Gulong shale oil in Daqing Oilfield, NE China. Pet Explor Dev 2021;48(3):527–40.
[4] Wang GY, Wang FL, Zhao B, Sun GX, Meng QA, Wang YZ, et al. Exploration and development situation and development strategy of Daqing Oilfield Company. China Pet Explor 2021;26:45–63.
[5] Wang YH, Liang JP, Zhang JY, Zhao B, Zhao Y, Liu X, et al. Resource potential and exploration direction of Gulong shale oil in Songliao Basin. Pet Geol Oilfield Dev Daqing 2020;39:20–34. Chinese.
[6] Xie JR. Petroleum. Shanghai: The Commercial Press; 1929. Chinese.
[7] Jin ZJ, Bai RZ, Gao B, Li MW. Has China ushered in the shale oil and gas revolution? Oil Gas Geol 2019;40:451–8. Chinese.
[8] Jin ZJ, Zhu RK, Liang XP, Shen YQ. Several issues worthy of attention in current lacustrine shale oil exploration and development. Pet Explor Dev 2021;48(6):1471–84.
[9] Zhao WZ, Hu SY, Hou LH, Yang T, Li X, Guo BC, et al. Types and resource potential of continental shale oil in China and its boundary with tight oil. Pet Explor Dev 2020;47(1):1–11.
[10] Zhao WZ, Zhu RK, Hu SY, Hou LH, Wu ST. Accumulation contribution differences between lacustrine organic-rich shales and mudstones and their significance in shale oil evaluation. Pet Explor Dev 2020;47(6):1160–71.
[11] Ma YS, Cai XY, Zhao PR, Hu ZQ, Liu HM, Gao B, et al. Geological characteristics and exploration practices of continental shale oil in China. Acta Geol Sin 2022;96(1):155–71. Chinese.
[12] Gao RQ. Characteristics of petroleum generation and expulsion in abnormal pressure shale zones and the formation of fracture shale reservoirs. Pet Geol Oilfield Dev Daqing 1984;3:160–7. Chinese.
[13] Jiang S, Tang XL, Steve O, Thomas A. Enrichment factors and current misunderstanding of shale oil and gas: case study of shales in US, Argentina and China. Earth Sci 2017;42(7):1083–91. Chinese.
[14] Li MW, Ma XX, Jiang QG, Li ZM, Pang XQ, Zhang CC. Enlightenment from formation conditions and enrichment characteristics of marine shale oil in North America. Pet Geol Recovery Effic 2019;26(1):13–28. Chinese.
[15] Bai GP, Qiu HH, Deng ZZ, Wang WY, Chen J. Distribution and main controls for shale oil resources in USA. Pet Geol Exp 2020;42(4):524–32. Chinese.
[16] Fu JH, Li SX, Niu XB, Deng XQ, Zhou XP. Geological characteristics and exploration of shale oil in Chang 7 Member of Triassic Yanchang Formation, Ordos Basin, NW China. Pet Explor Dev 2020;47(5):931–45.
[17] Fu ST, Jin ZJ, Fu JH, Li SX, Yang WW. Transformation of understanding from tight oil to shale oil in the Member 7 of Yanchang Formation in Ordos Basin

and its significance of exploration and development. Acta Petrol Sin 2021;42:561–9. Chinese.
[18] Zhi DM, Tang Y, Yang ZF, Guo XG, Zheng ML, Wan M, et al. Geological characteristics and accumulation mechanism of continental shale oil in Jimusaer Sag, Junggar Basin. Oil Gas Geol 2019;40:524–36. Chinese.
[19] Zhao XZ, Zhou LH, Pu XG, Jin FM, Han WZ, Xiao DQ, et al. Geological characteristics of shale rock system and shale oil exploration breakthrough in a lacustrine basin: a case study from the Paleogene 1st sub-member of Kong 2 Member in Cangdong Sag, Bohai Bay Basin, China. Pet Explor Dev 2018;45(3):377–88.
[20] Zhao XZ, Zhou LH, Pu XG, Jin FM, Shi ZN, Han WZ, et al. Formation conditions and enrichment model of retained petroleum in lacustrine shale: a case study of the Paleogene in Huanghua depression, Bohai Bay Basin, China. Pet Explor Dev 2020;47(5):916–30.
[21] Li MY, Wu ST, Hu SY, Zhu RK, Meng SW, Yang JR. Lamination texture and its effects on reservoir and geochemical properties of the Paleogene Kongdian Formation in the Cangdong Sag, Bohai Bay Basin, China. Minerals 2021;11(12):1360.
[22] Song GQ, Xu XY, Li Z, Wang XH. Factors controlling oil production from Paleogene shale in Jiyang depression. Oil Gas Geol 2015;36:463–71. Chinese.
[23] Liu HM, Yu BS, Xie ZH, Han SY, Shen ZH, Bai CY. Characteristics and implications of micro-lithofacies in lacustrine basin organic-rich shale: a case study of Jiyang depression, Bohai Bay Basin. Acta Petrol Sin 2018;39:1328–43. Chinese.
[24] Li GX, Zhu RK, Zhang YS, Chen Y, Cui JW, Jiang YH, et al. Geological characteristics, evaluation criteria and discovery significance of Paleogene Yingxiongling shale oil in Qaidam Basin, NW China. Pet Explor Dev 2022;49(1):21–36.
[25] Zou CN, Yang Z, Wang HY, Dong DZ, Liu HL, Shi ZS, et al. "Exploring petroleum inside source kitchen": Jurassic unconventional giant shale oil & gas field in Sichuan Basin, China. Acta Geol Sin 2019;93:1551–62. Chinese.
[26] He WY, He HQ, Wang YH, Cui BW, Meng QA, Guo XJ, et al. Major breakthrough and significance of shale oil of the Jurassic Lianggaoshan Formation in Well Ping'an 1 in northeastern Sichuan Basin, China. Pet Explor 2022;27:40–9.
[27] He WY, Meng QA, Zhang JY. Controlling factors and their classification-evaluation of Gulong shale oil enrichment in Songliao Basin. Pet Geol Oilfield Dev Daqing 2021;40:1–12. Chinese.
[28] He WY, Meng QA, Feng ZH, Zhang JY, Wang R. *In-situ* accumulation theory and exploration & development practice of Gulong shale oil in Songliao Basin. Acta Petrol Sin 2022;43:1–14. Chinese.
[29] He WY, Cui BW, Wang FL, Wang YZ, Meng QA, Zhang JY, et al. Study on reservoir spaces and oil states of the Cretaceous Qingshankou Formation in Gulong Sag, Songliao Basin. Geol Rev 2022;68:693–741. Chinese.
[30] Hua GL, Wu ST, Zhang JY, Yu XH, Guan MD, Zhao Y, et al. Laminar structure differences and heterogeneities in reservoirs in continental organic-rich shales: the Cretaceous Nenjiang Formation in the Songliao Basin. Interpretation 2022;10(3):SD89–106.
[31] Cai Y, Zhu RK, Luo Z, Wu ST, Zhang TS, Liu C, et al. Lithofacies and source rock quality of organic-rich shales in the Cretaceous Qingshankou Formation, Songliao Basin, NE China. Minerals 2022;12(4):465.
[32] Feng ZH, Fang W, Wang X, Huang CY, Huo QL, Zhang JH, et al. Microfossils and molecular records in oil shales of the Songliao Basin and implications for paleo-depositional environment. Sci China Ser D Earth Sci 2009;52:1559.
[33] Feng ZH, Fang W, Li ZG, Wang X, Huo QL, Huang CY, et al. Depositional environment of terrestrial petroleum source rocks and geochemical indicators in the Songliao Basin. Sci China Earth Sci 2011;54(9):1304–17.
[34] Feng ZH, Huo QL, Zeng HS, Wang YZ, Jia YS. Organic matter compositions and organic pore evolution in Gulong shale of Songliao Basin. Pet Geol Oilfield Dev Daqing 2021;40:40–55. Chinese.
[35] Cao H, He W, Chen F, Shan X, Kong D, Hou Q, et al. Integrated chemostratigraphy ($\delta^{13}C$-$\delta^{34}S$-$\delta^{15}N$) constrains Cretaceous lacustrine anoxic events triggered by marine sulfate input. Chem Geol 2021;559:119912.
[36] Zheng GD, Meng QT, Liu ZJ. Paleolimnological information of oil shale in 1st member of Qingshankou Formation in northern Songliao Basin. J Jilin Univ 2020;50(2):392–404. Chinese.
[37] Yang WL, Gao RQ, Guo QF, Liu YG. Continental petroleum generation, migration and accumulation in the Songliao Basin. Harbin: Heilongjiang Science & Technology Press; 1985. Chinese.
[38] Gao RQ, Cai XY. Forming conditions and distribution of petroleum fields in the Songliao Basin. Beijing: Petroleum Industry Press; 1997. Chinese.
[39] Hou QJ, Feng ZQ, Feng ZH. Continental petroleum geology in the Songliao Basin. Beijing: Petroleum Industry Press; 2009. Chinese.
[40] Tissot BP, Welte DH. Petroleum formation and occurrence. 2nd ed. Berlin: Springer verlag; 1984.
[41] Chen JP, Sun YG, Zhong NN, Huang ZK, Deng CP, Xie LJ, et al. The efficiency and model of petroleum expulsion from the lacustrine source rocks within geological frame. Acta Geol Sin 2014;88:2005–32. Chinese.
[42] Sweeney JJ, Burnham AK. Evaluation of a simple model of vitrinite reflectance based on chemical kinetics. AAPG Bull 1990;74(10):1559–70.
[43] Wilson MJ, Wilson L, Shaldybin MV. Clay mineralogy and unconventional hydrocarbon shale reservoirs in the USA. II. Implications of predominantly illitic clays on the physico–chemical properties of shales. Earth Sci Rev 2016;158:1–8.
[44] Milliken KL, Rudnicki M, Awwiller DN, Zhang TW. Organic matter-hosted pore system, Marcellus Formation (Devonian), Pennsylvania. AAPG Bull 2013;97:177–200.
[45] Wu ST, Yang Z, Zhai XF, Cui JW, Bai LS, Pan SQ, et al. An experimental study of organic matter, minerals and porosity evolution in shales within high-temperature and high-pressure constraints. Mar Pet Geol 2019;102:377–90.
[46] Julia FWG, Stephen EL, Jon EO, Peter E, András F. Natural fractures in shale: a review and new observations. AAPG Bull 2014;98(11):2165–216.
[47] Pommer M, Milliken K. Pore types and pore-size distributions across thermal maturity, Eagle Ford Formation, southern Texas. AAPG Bull 2015;99(9):1713–44.
[48] Jia CZ, Pang XQ, Song Y. The mechanism of unconventional hydrocarbon formation: hydrocarbon self-sealing and intermolecular forces. Pet Explor Dev 2021;48(3):507–26.
[49] Hu T, Pang XQ, Jiang FJ, Wang QF, Liu XH, Wang Z, et al. Movable oil content evaluation of lacustrine organic-rich shales: methods and a novel quantitative evaluation model. Earth Sci Rev 2021;214:103545.
[50] Han YJ, Horsfield B, Wirth R, Mahlstedt N, Bernard S. Oil retention and porosity evolution in organic-rich shales. AAPG Bull 2017;101(06):807–27.
[51] Han YJ, Horsfield B, Mahlstedt N, Wirth R, Curry DJ, LaReau H. Factors controlling source and reservoir characteristics in the Niobrara shale oil system, Denver Basin. AAPG Bull 2019;103(9):2045–72.
[52] Gorynski KE, Tobey MH, Enriquez DA, Smagala TM, Dreger JL, Newhart RE. Quantification and characterization of hydrocarbon filled porosity in oil-rich shales using integrated thermal extraction, pyrolysis, and solvent extraction. AAPG Bull 2019;103(3):723–44.
[53] Romero-Sarmiento MF. A quick analytical approach to estimate both free versus sorbed hydrocarbon contents in liquid-rich source rocks. AAPG Bull 2019;103(9):2031–43.